STM Program 2014

Assessment of crustal deformation around the Pärvie post-glacial fault in Lapland Sweden, using a hybrid interferometric approach.

M.MANTOVANI

matteo.mantovani@irpi.cnr.it
Tel: +39 049 8295801
Fax: +39 049 8295827
ISTITUTO DI RICERCA PER LA PROTEZIONE IDROGEOLOGICA (CNR-IRPI). Corso Stati Uniti, 4 35127 Padova (Italy).

Introduction

Northern Fennoscandia bears witness of the Pleistocene glaciation in the form of a series of large faults. The largest, known as Pärvie, consists of a linear series of scarps, almost all of them west-facing and together forming a north-north-east trending, 155 km long fault line. These faults have been found to be associated with major earthquakes, presumably occurring around 10,000 years ago in a single event, causing displacements on the order of 10 m. Post-glacial and End-glacial faults (PGF's) seem to be unique for Fennoscandia, although ice sheets have been present in many more locations on the earth. Given that they were generated shortly before or after the ice margin had moved past them, it is not easy to understand that they do not appear elsewhere, neither near e.g. the Laurentide ice sheet region nor at locations of present melting (Greenland, West-Antarctica, Alaska). Seismological evidence from the SNSN (Swedish National Seismic Network) shows that there is still noticeable seismic activity. Apart from seismicity, no information available on the state of activity of the Pärvie fault and no surface deformations data have ever been collected. The length of the fault and its location, mainly over not easily accessible areas, make the traditional monitoring techniques unfeasible and ineffective. The authors successfully applied DInSAR (Differential Synthetic Aperture Radar Interferometry) to detect deformations around the fault area, isolating fringes along different sectors (Mantovani & Scherneck, 2013). In the framework of the Short Term Mobility Program we aimed at implementing a hybrid interferometric approach, based on conventional two-pass SAR differential interferometry (DInSAR), Short Baselines Subsets (SBAS) and Persistent Scatterers (PS) techniques such as the Interferometric Point Target Analysis (IPTA) to assess the creep rate along the entire length of the fault.

The Pärvie fault

During recession of the Pleistocene ice sheet, major faults became engaged with estimated seismic magnitudes beyond M8 (Bäckblom and Munier, 2002). The region where several of these faults occur is in Northern Bothnia, Lapland, Sweden and bordering areas of Norway and Finland. It appears that these faults respond to ongoing stress changes and it is suggested that they might accumulate a part of the postglacial rebound strain in their environment. Intra-plate structures of this extent and young age are very rare in the continental crust. Due to their young age, the conditions on the fault plane at depth could still be affected by the heat release during the major shock, making the fault zone admissible to enhanced creep as compared to the regular

lithosphere sections. The fact that the traces and heights of the individual fault segments belonging to a certain fault set, as well as the gaps in between the separate segments, appear to be largely governed by the structures and composition of the superficial bedrock, indicates that more continuous faulting and fault rupture must occur at depth. The main Pärvie fault consists of a linear series of fault scarps, almost all of them west-facing and together forming a north-north-east trending, 155 km long fault line (Figure 1).

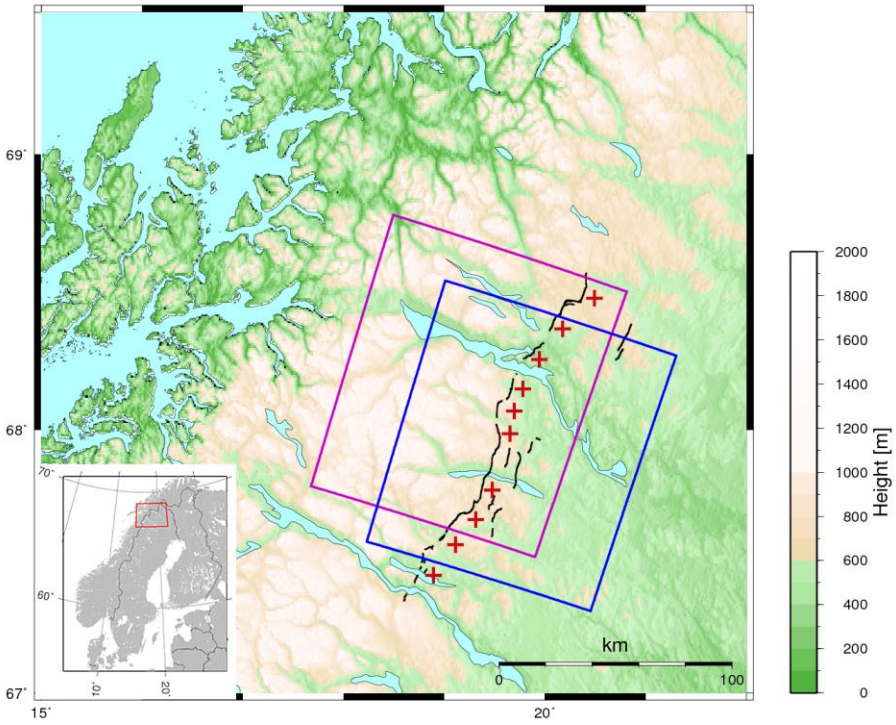

Figure 1. *The Pärvie fault system (black lines). Red plus symbols indicate the uplifted blocks while blue and purple squares represents the perimeters of track 480-frame 2223 and track 251-frame 223 SAR scenes, respectively (from Mantovani & Scherneck 2013).*

Only in a lesser part of its stretch the fault appears to fan out towards the surface to create parallel escarpments. Bedrock exposures occur rather frequently along parts of the fault, and at several locations overhanging cliffs indicates reverse movement on steeply dipping fault planes. This is in itself unusual in tectonics, as steeply dipping fault planes are commonly associated with normal, not reverse fault slip. Field observation and photogrammetric measurements indicate that fault scarp heights generally vary between 3 m and 10 m (Figure 2), but locally somewhat greater heights were measured (Lagerbäck & Witschard 1983; Lagerbäck & Sundh 2008). At varying distances to the east of the master fault there is a number of subsidiary fault scarps, almost all of them east facing, i.e. opposite to the master fault. The generation of the mainly competent earthquake has been attributed to large loading stress gradients at the time of the Pleistocene ice sheet retreat. The area is still undergoing vertical and horizontal deformation as an effect of glacial isostatic adjustment. These motions have been observed using continuous GPS in the permanent GNSS networks of the Nordic countries. Nevertheless the fault structure is on a spatial scale that is difficult to resolve with the ~200 km mesh width GNSS network.

Signs of persistent weakness are found in a higher-than-average contemporary seismicity as observed by the SNSN (Swedish National Seismic Network) (Figure 3). Due to their locations in remote areas, no excavations have been carried out across any of the scarps belonging to the Pärvie fault system.

Figure 2. *Aerial view of the Pärvie fault scarp from 300 m above ground and looking to northeast (photograph by Hans-Georg Scherneck).*

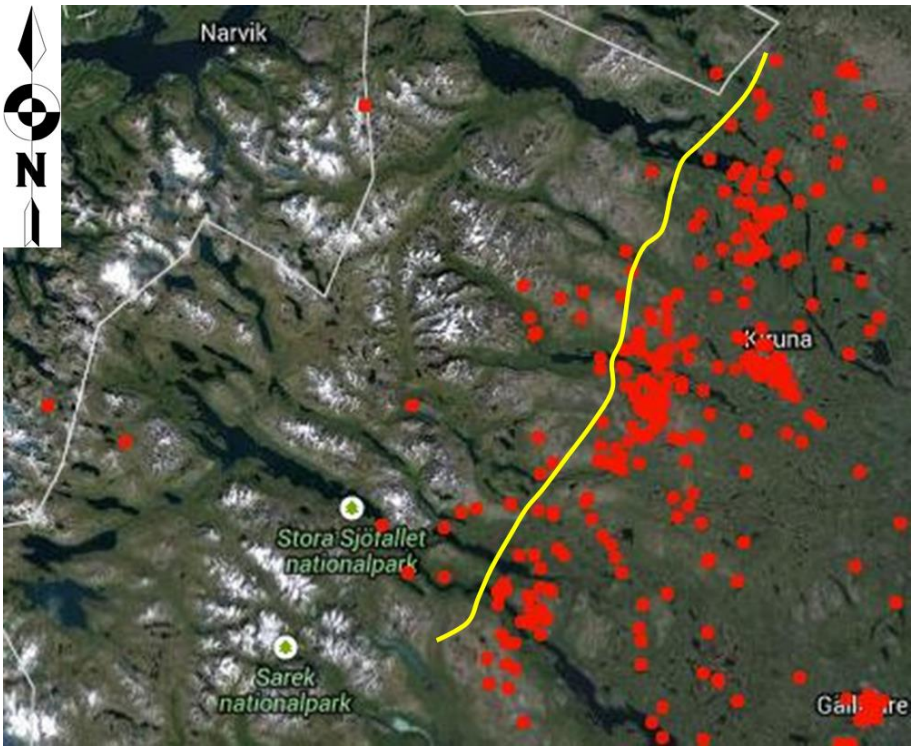

Figure 3. *Pärvie fault (yellow line) and earthquake epicentres (red dots) recorded at SNSN, Uppsala university, between April 2000 and May 2009 (http://snsn.geo.uu.se).*

DInSAR technique

DInSAR offers the possibility to measure deformation at centimetre to millimetre accuracy over long time periods in large inaccessible areas coupling the precision of geodetic measurements with the advantages of remote sensing techniques (Bamler & Hartl 1998). Nevertheless retrieving displacements that are supposedly in the order of few millimeters or less per year, over the Pärvie fault is not an easy task. The major limiting factor is the presence of snow on the ground for about nine months per year (Figure 4).

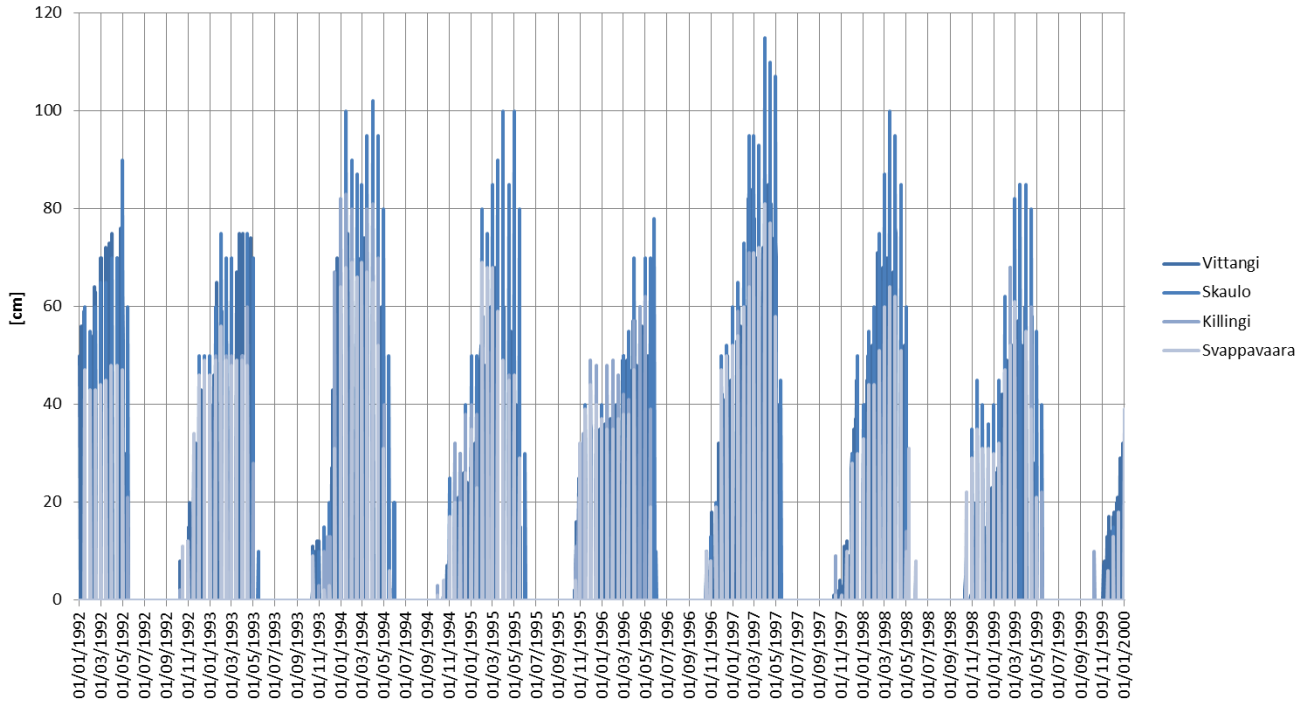

Figure 4. *Snow heights recorded by 4 meteorological stations around the study area between January 1992 and January 2000.*

This strongly reduces the number of images suitable for interferometric purposes and hence the possibility to detect very slow deformations. Despite all the limiting factors some promising results have been achieved applying DInSAR technique. A study recently published by Mantovani & Scherneck (2013) clearly showed deformation fringes related to the activity of Pärvie fault (Figure 5). Interferometric patterns, that can be reasonably attributed to active landslides, were also detected with the interferometric analysis (Figure 6).

DInSAR analysis: results and discussion

DInSAR analysis lead to the conclusion that the Pärvie fault is active, and the component of the deformation along the line of sight (LOS) of the sensor (i.e. 23° with respect to the vertical) is quantifiable in few millimetres per year. The fact that fringes related to displacement are visible in three independent datasets (see Figure 5), covering different time periods and they are consistent and increasing showed that they can't be related to a single episodic event (i.e. earthquakes) but they must be generated by some other kind of phenomena (e.g. creep). Moreover under the assumption that the displacements occurred along the vertical direction, the suggested reverse behavior is confirmed.

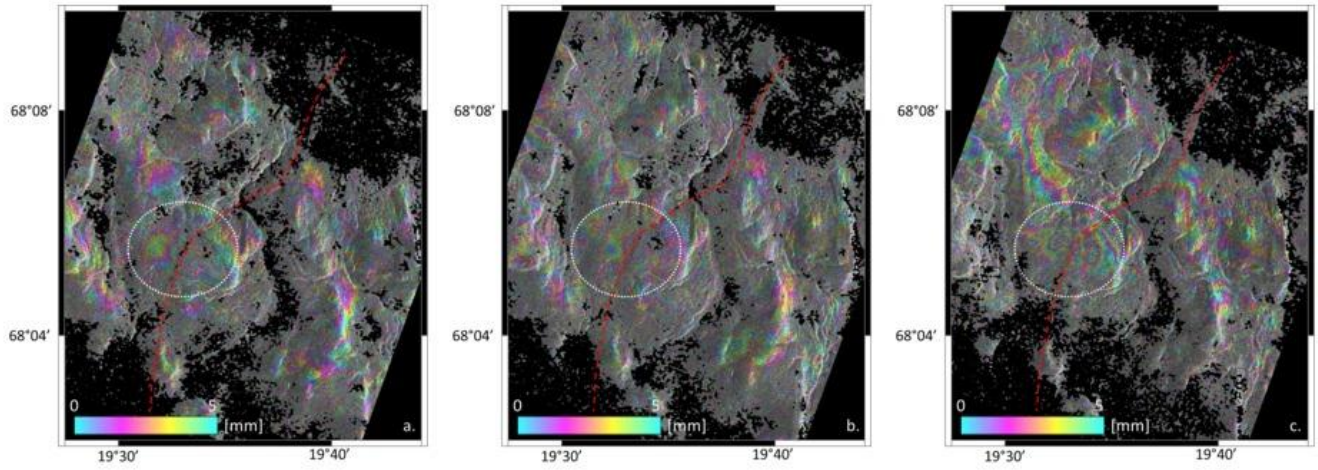

Figure 5. *Differential interferograms generated from images: 1992-09-17 and 1996-07-07, ERS track 480 (a); 1992-07-28 and 1995-07-06, ERS track 251 (b); 2007-08-03 and 2009-08-07, ENVISAT track 251 (c). The red line represents the segments of the Pärvie fault, the dotted white ellipse highlights the deformation area (Mantovani & Scherneck 2013).*

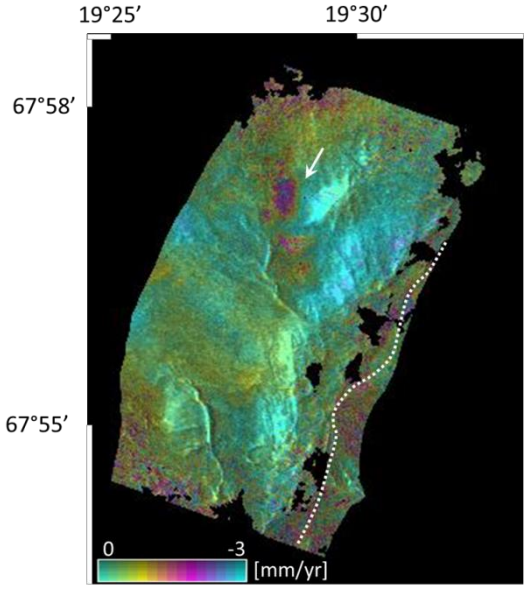

Figure 6. *Stacked interferograms superimposed to a geocoded intensity image of a segments of the Pärvie fault (white dotted line). White arrow highlight the deformations due to a landslide. One colour cycle correspond to a line of sight deformation rate of 3 mm/yr*

Geomorphological interpretation of aerial photographs (Lagerbäck and Witschard, 1983) detected a total of about 250 landslides in northern Sweden, most of them in the Norrbotten county, close to the Finnish border. The peculiarity of this fact is that this area cannot be considered prone to landslide neither from a geological nor from a topographical point of view. Quaternary deposits, mainly composed of sandy tills are not expected to slide or flow under normal circumstances, especially not along very gentle slopes of only a few degrees (Lagerbäck & Sundh, 2008). Since the majority of these landslides occur adjacent to fault scarps, it is believed that the slope failures have been triggered by seismically induced liquefaction processes. Kujansuu (1972)

suggested for the first time the possibility that earthquakes associated with the supposed recent faulting in Finnish Lapland had triggered landslides in the vicinity of the fault scarps, and Lagerbäck and Witschard (1983) strengthened this hypothesis observing similar correlations in the Norrbotten county. In this context the landslides detected with the DInSAR analysis supported the hypothesis that the Pärvie generated after the retirement of the glaciers.

Hybrid approach implementation

DInSAR analysis offered the possibility to detect deformation patterns and to assess the cumulative displacements occurred between two acquisitions over some stretches of the Pärvie fault. In the attempt to derive the deformation time series for the entire faults length and to follow its temporal evolution, we tried to implemented an interferometric hybrid approach. Persistent Scatters Interferometry (PSI) (Ferretti at al., 2001) and Short Baseline Subset (SBAS) techniques (Berardino et al., 2002) are the only methods that can reduce the atmospheric disturbances and provide accurate and reliable results in terms of crustal deformations. Yet, the absence of man-made structures in the remote regions of Lapland where the fault runs, is a well-known limiting factor in the application of the PSI technique. In our analysis the amount of natural point-like reflectors was rather low. The crystalline bedrock that expose frequently and cover wide areas of the investigated region behave like distributed scatterers (DS). Ferretti et al. (2011) demonstrated that, taking into account the statistical behavior of the DS and 'squeezing' the associated coherence matrix, a vector of optimum phase values can be provided, hence the possibility to perform a traditional PS analysis over DS as well. The SqueeSAR algorithm is a trademark registered by TRE (TeleRilevamento Europa) and the patent is pending. We developed a hybrid DInSAR procedure that—after multi-looking the phase of a stack of short baseline interferograms and using the IPTA (Interferometric Point Target Analysis) processing—can provide similar results to the SqueeSAR technique. It is clear that the possibility to extract geophysical parameters (i.e. deformation rates) is of primary importance for our research purposes, and that a high density of surface representatives (DS, PS) is the key to this end. In examples for similar terrains, the Ferretti group could demonstrate a gain of a factor of three when adding DS's to the PS set.

In our approach we used images with short spatial baselines in order to optimize the coherence and minimize the topography relate phase errors. Phase noise was then strongly reduced after averaging the images over a large number of complex looks (e.g. 4 in rage and 20 in azimuth) obtaining a pixel size of about 80x80 m.

The processing steps of the approach can be summarized as follows:

1. Co-registration of the images to a single reference.
2. Two pass differential interferometry processing between selected pair of images using an external DEM (Digital Elevation Model) to reduce the topographic phase term (DInSAR).
3. Heights updating based on very long baseline pair with short time interval (i.e. tandem pair).
4. Slope adaptive common band filtering.
5. Baseline refinement.
6. Estimation and subtraction of the topography related atmospheric phase term.
7. Derivation of a single reference time series using Singular Value Decomposition (SVD)
8. Extrapolation of the least-square solution for phase time series at every pixel location.

Hybrid approach validation over the Kiruna test site

In order to validate the method we applied the analysis over the test site of Kiruna. The city, that is located few kilometers easterly to the Pärvie fault, is affected by subsidence due to presence of the world's largest underground iron ore mine. It is estimated that the effects of the expansion of the mining activity will affect 1,800 people living in Kiruna in the next years. The deformation prognosis is so severe and the related hazard so high that the Swedish Authorities are planning to re-locate the entire city away from the mine (Figure 7).

Figure 7. *Deformation prognosis of the Kiruna mining inducted subsidence.*

The interferometric analysis over the city of Kiruna was performed using ERS images acquired from track 480-frame 2223. Figure 8 shows the cumulative deformation inducted in 280 days by sublevel caving on the mine hangingwall. The colour coded image is the results of DInSAR processing of two ERS images acquired between August 1992 and May 1993. Several other interferograms, with increasing temporal baseline, were generated in the attempt to assess the evolution of subsidence around the mine. As the temporal baseline increases the increment of the deformation and its migration towards the city becomes evident until the noise makes the interpretation of the interferometric phase harder and less accurate (Figure 9). The small number of natural radar reflectors around the mining area did not allowed to perform a PSI analysis, that was restricted to the city over 1062 point targets. The colour coded deformation map, superimposed to the amplitude image of Kiruna is reported on Figure 10.

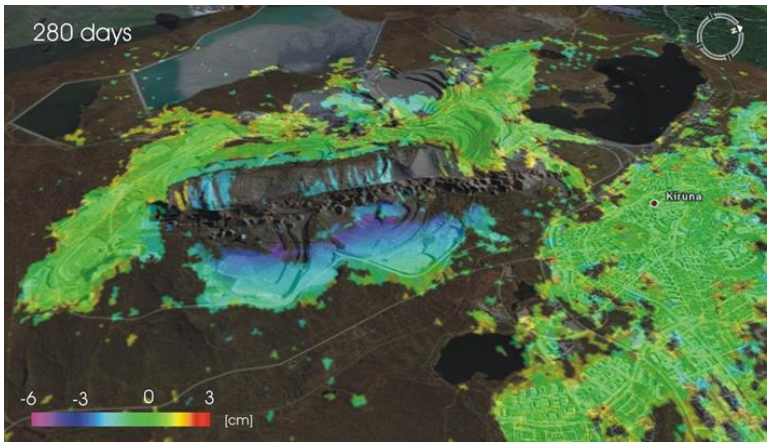

Figure 8. *Line of sight (LOS) displacements measured from an interferogram generated by images acquired 280 days apart (August 1992 – May 1993) superimposed to a Google Earth image of Kiruna.*

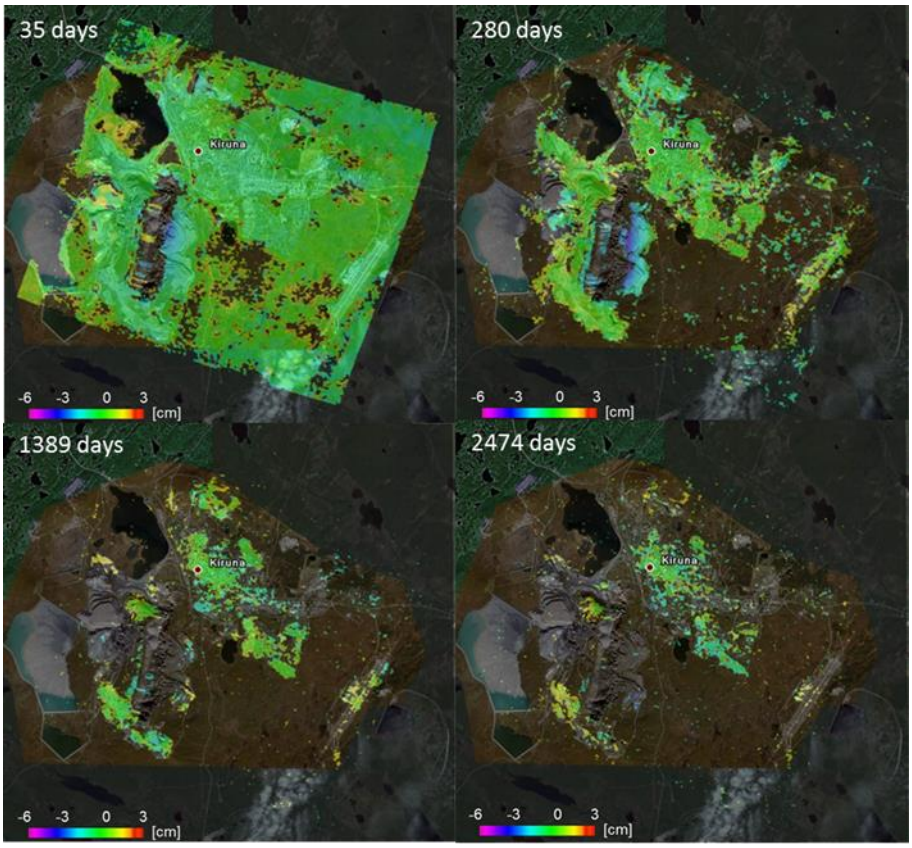

Figure 9. *Line of sight (LOS) displacements measured from 4 different interferograms with increasing temporal baseline and superimposed to a Google Earth image of Kiruna.*

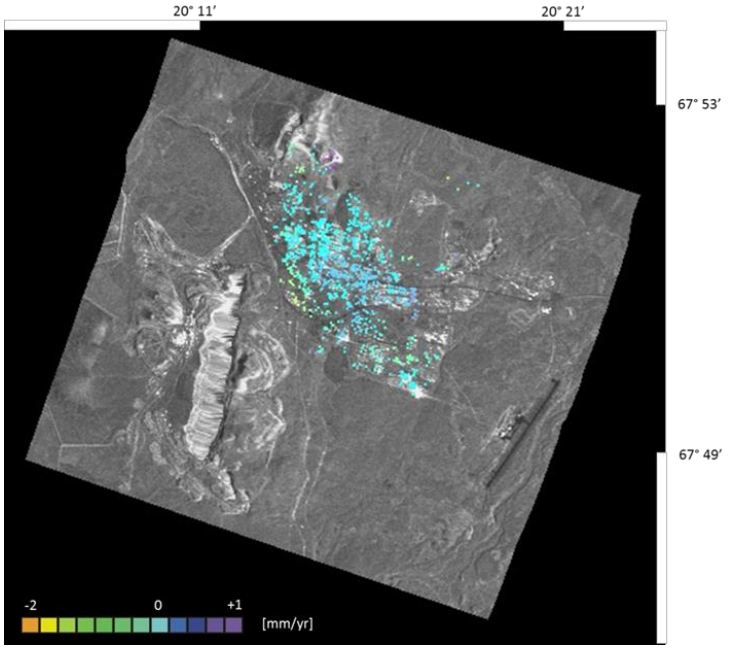

Figure 10. *Amplitude image of Kiruna with PS location. Blue targets are stable, yellow points are subsiding.*

The maximum deformation rates measured during the seven years investigation period (1992-1999) are in the order of 1÷2 mm/yr. Finally the hybrid approach was applied. Time series of the mining inducted subsidence are shown in Figure 11.

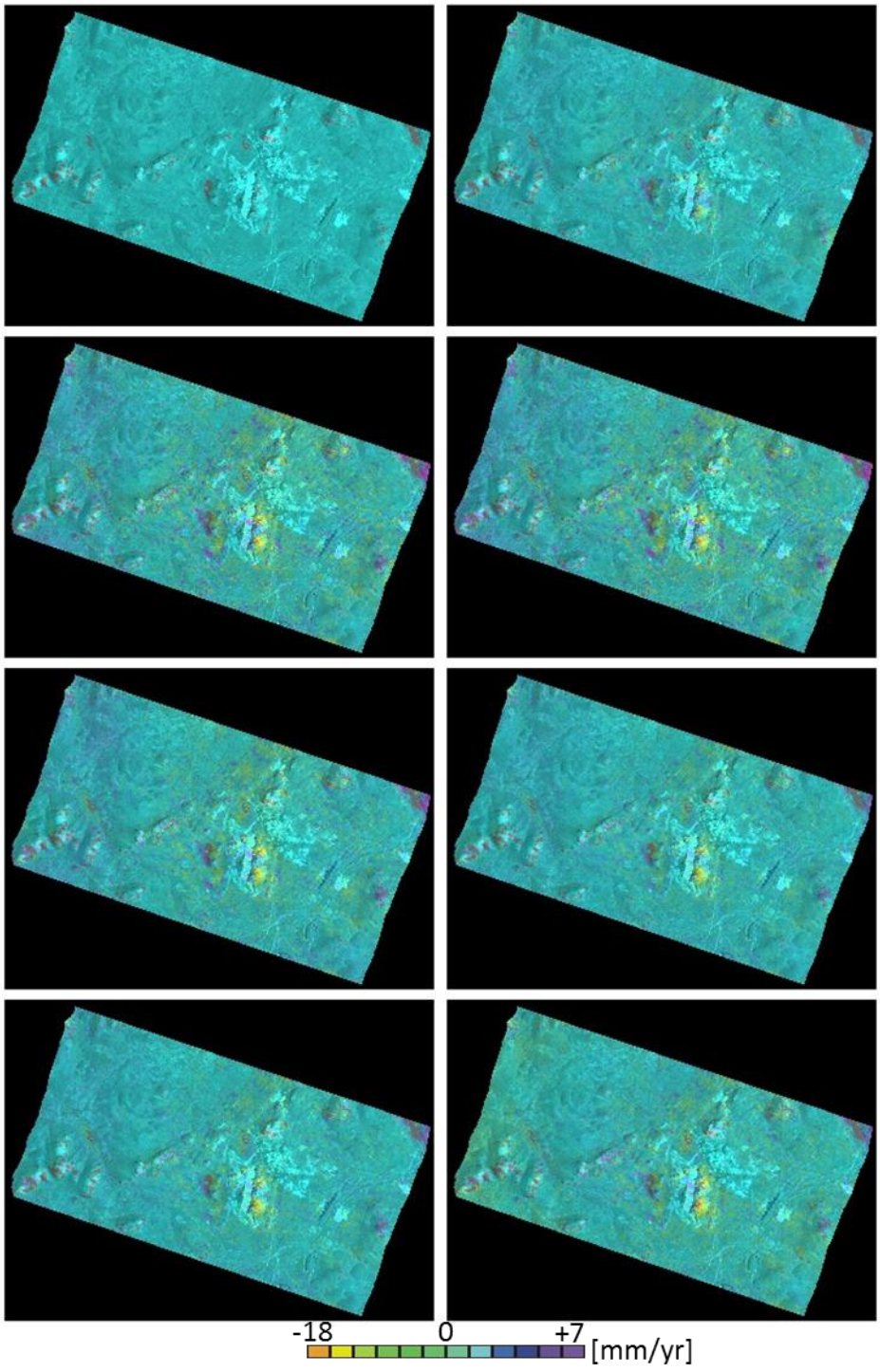

Figure 11. *Deformation time series (LOS component) estimated between September 17 1992 and August 1 1999.*

Despite the poorer resolution compared to former images we were able to extract phase information almost anywhere in the framed area. Deformation time series for 3 characteristic points are resumed in Figure 12. These results, that are consistent with those retrieved from the DInSAR and PS analysis, provide evidences of the reliability of the hybrid approach. Through the application of this method we were able to extract deformation rates from a high density of surface representatives.

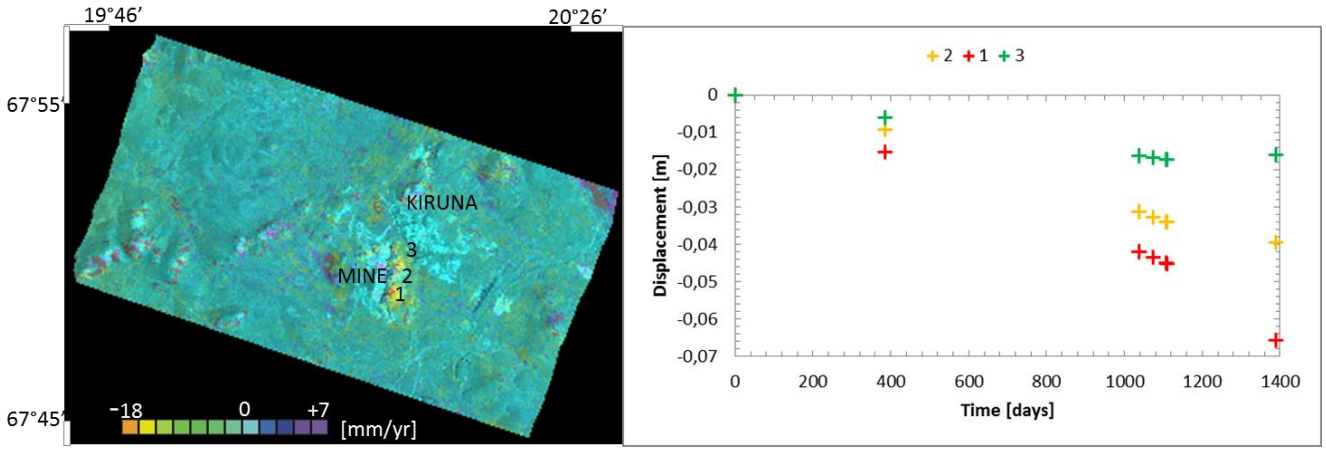

Figure 12. *Deformation time series (LOS componenet) for three characteristic points. Times are indicated in days after September 17 1992 .*

Hybrid approach application to the Pärvie fault

We applied the hybrid approach on three dataset acquired on two parallel descending orbits by ERS and ENVISAT satellites whose details are resumed on Table 1.

Table 1. *List of SAR images used in the interferometric processing.*

ERS-1/2		ERS-1/2				ENVISAT	
TRACK 480-FRAME 2223		TRACK 251-FRAME 2223				TRACK 251-FRAME 2223	
n.	Acquisition Date	n.	Acquisition Date	n.	Acquisition Date	n.	Acquisition Date
1	13/08/1992	1	23/06/1992	16	15/08/1997	1	03/10/2003
2	17/09/1992	2	28/07/1992	17	19/09/1997	2	09/07/2004
3	20/05/1993	3	01/09/1992	18	11/06/1999	3	13/08/2004
4	29/07/1993	4	06/10/1992	19	16/07/1999	4	22/10/2004
5	07/10/1993	5	13/07/1993	20	20/08/1999	5	29/07/2005
6	17/06/1995	6	21/09/1993	21	24/09/1999	6	22/09/2006
7	22/07/1995	7	01/06/1995	22	26/05/2000	7	27/10/2006
8	23/07/1995	8	02/06/1995			8	25/05/2007
9	26/08/1995	9	06/07/1995			9	03/08/2007
10	30/09/1995	10	07/07/1995			10	07/09/2007
11	01/10/1995	11	14/09/1995			11	07/08/2009
12	07/07/1996	12	15/09/1995			12	11/09/2009
13	27/06/1999	13	19/10/1995				
14	01/08/1999	14	20/10/1995				
15	05/09/1999	15	25/07/1996				

We constrained the perpendicular baseline at a value of 150 m and the temporal in 1095 days (i.e. 3 years). Figure 13 shows the connection graphs of the three datasets. As he can be noticed the constraints are unfortunately satisfied just for few images. We used tandem datasets to improve the topographic height estimation and removed the height related phase delay using a linear regression model. Each differential interferogram was referenced to the time of the earliest scene in the series and by definition, the deformation was set to 0 at the initial epoch for the series. We used the Single Value Decomposition to obtain the least-squares solution for the phase time-series. We also produced a simulated deformation phase for each of the input interferograms using the estimated deformation phase-time series. These phase terms were hence subtracted from the original interferograms leaving a combination of residual baseline phase, noise, and phase unwrapping errors that were removed in the second iteration of the process (Wegmüller et al., 2009).

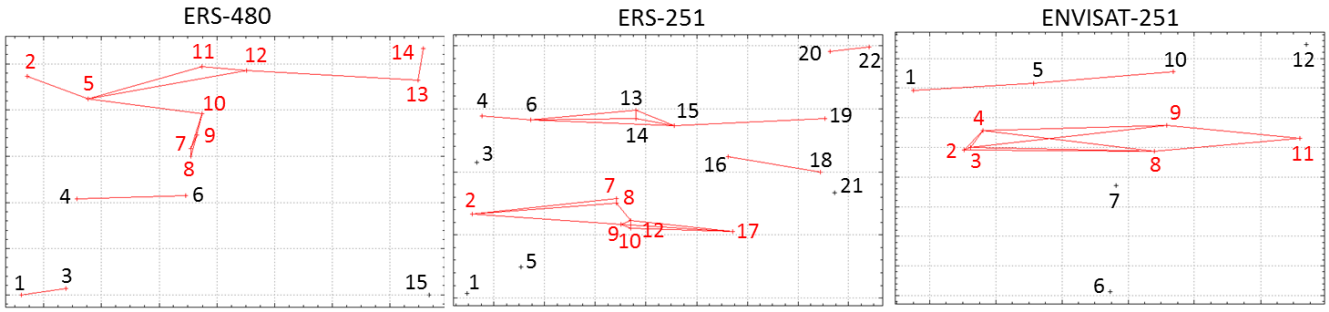

Figure 13. *Connection graphs for the three datasets used in the analysis with the baseline constraint equal to 150 m for the spatial (y axis) and 3 yr for the temporal (x axis). Unfortunately the redundancy between pairs and connection is very poor for all the datasets. Red numbers identify the images used in the processing.*

Discussion and conclusions

Beside the good results achieved in the validation test over the site of Kiruna, the hybrid methodology failed to detect deformation rates along the Pärvie fault (Figure 14,15,16). The reason resides in the small number and the poor temporal sampling of the available datasets that did not allow to significantly reduce the phase noise. In the best configuration (ENVISAT track 251) we obtained 5 time series with just 10 pairs of images (e.g. very few interferograms represented with a red line in Figure 13 contain information from each of the images). With such a small redundancy it is hard to isolate extremely slow creep deformations, especially in boreal regions where the snow coverage on the ground is an issue. Nevertheless the hybrid approach implemented in this study seem to be the only alternative since the total absence of man-made structures makes PSI analysis unfeasible. Future research perspective will consider the application of this novel approach to datasets acquired by the latest ESA (European Space Agency) latest space-borne interferometric missions such as Sentinel that hopefully will provide a better coverage at high latitudes.

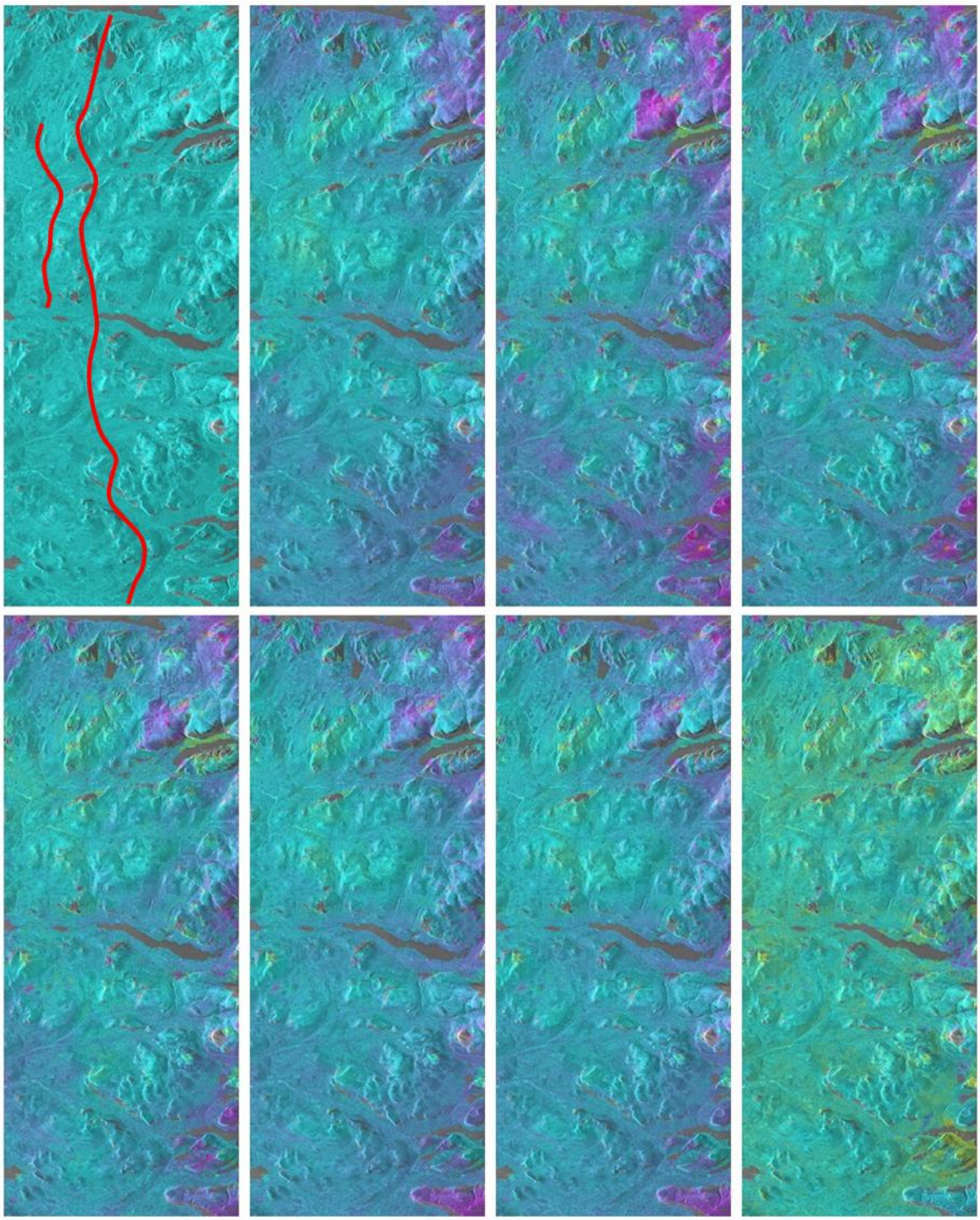

Figure 14. *Deformation time series (LOS component) in range-doppler coordinates estimated from ERS track 480-frame 2223, between September 17 1992 and August 1 1999.Pärvie fault is represented by the red lines.*

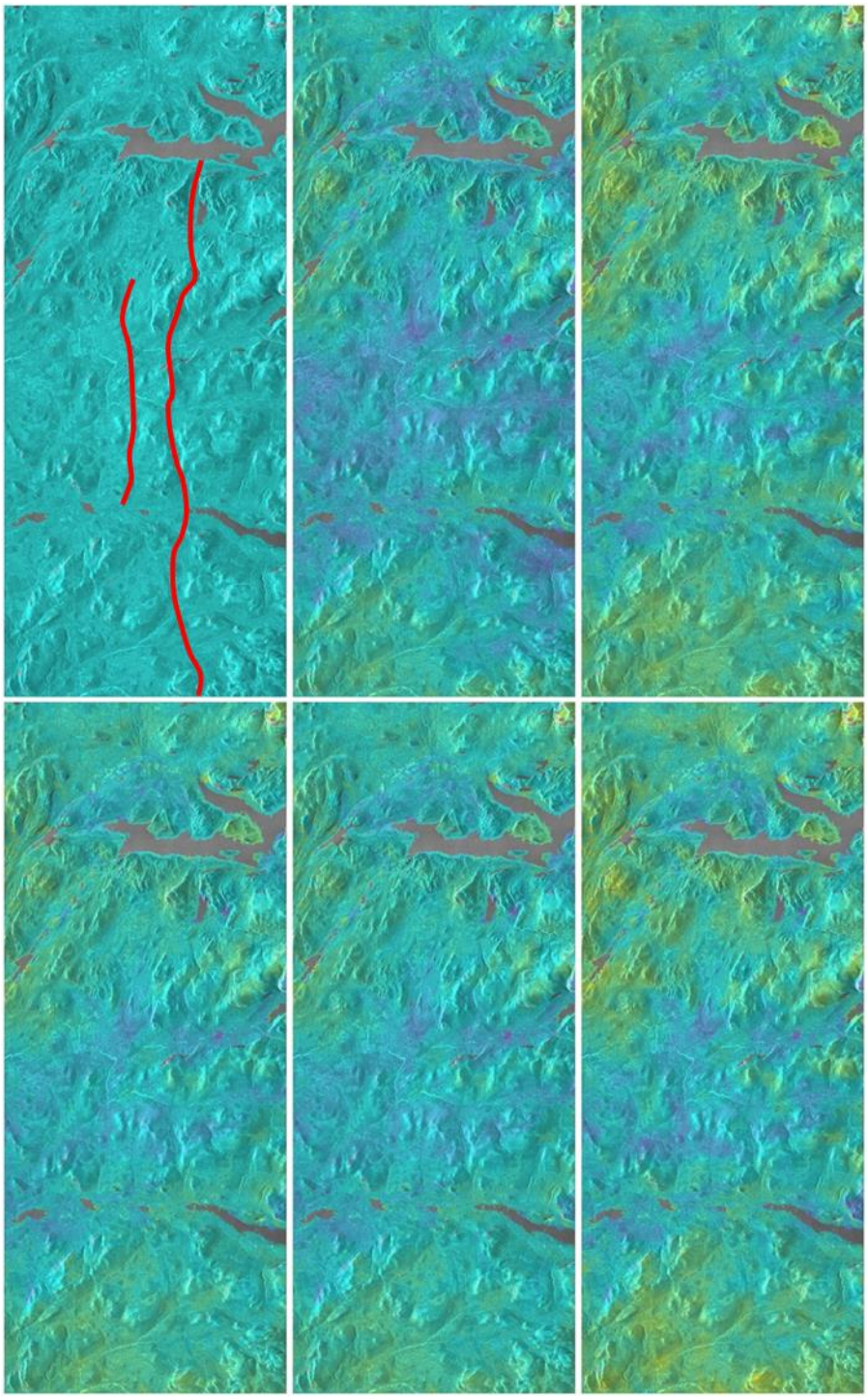

Figure 15. *Deformation time series (LOS component) in range-doppler coordinates estimated from ERS track 251-frame 2223, between July 28 1992 and September 19 1997.Pärvie fault is represented by the red lines.*

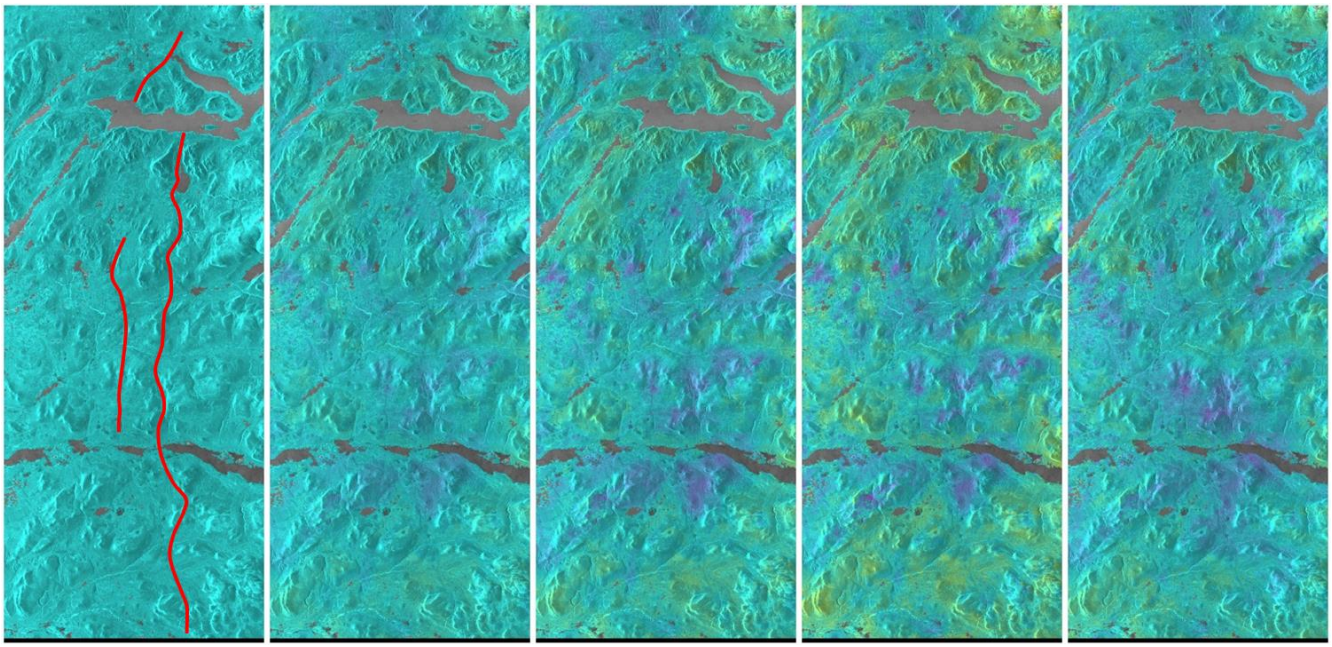

Figure 16. *Deformation time series (LOS component) in range-doppler coordinates estimated from ENVISAT track 251-frame 2223, between July 9 2004 and August 7 2009. Pärvie fault is represented by the red lines.*

Aknowledgements

This work, in the framework of the Short Mobility Term Program 2014, has been carried out in collaboration with Professor Hans-Georg Scherneck of the Chalmers University of Technology, Department of Earth and Space Sciences, Gothenburg, Sweden. The authors acknowledge European Space Agency for providing ERS and ENVISAT data (C1P.7559). SAR processing was performed using Gamma Software.

Bibliography

Bamler, R., Hartl, P., 1998. Synthetic aperture radar interferometry, Inverse Problems 14: R1-R54.

Berardino, P., Fornaro, G., Lanari, R., Sansosti, E., 2001. A New Algorithm for Surface Deformation Monitoring Based on Small Baseline Differential SAR Interferograms, IEEE Trans. Geosciences and Remote Sensing, 40 (11), pp. 2375-2383.

Bäckblom, G., Munier, R., 2002. Effects of earthquakes on the deep repository for spent fuel in Sweden based on case studies and preliminarymodel results. SKBTechnicalReport TR-02-24. Swedish Nuclear Fuel and Waste Management Co., Stockholm Sweden.

Ferretti, A., Prati, C., Rocca, F., 2001. Permanent Scatterers in SAR interferometry. IEEE Trans. Geosci. Remote Sens. 39 (1), pp. 8–20.

Ferretti, A., Fumagalli, A., Novali, F., Prati, C., Rocca, F., Rucci, A., 2011. A new algorithm for processing interferometric data-stacks: SqueeSAR. IEEE Transactions on Geosciences and Remote Sensing. 49, 3460-3470.

Kujansuu, R., 1972. On landslides in Finnish Lapland. Geological Survey of Finland, Bulletin 256, 22 pp.

Lagerbäck, R., Sundh, M., 2008. Early Holocene faulting and paleoseismicity in northern Sweden. SGU Research Paper C836, 80 pp.

Lagerbäck, R.,Witschard, F., 1983. Neotectonics in northern Sweden – geological investigations. SKBF/KBS Technical Report 83–58. Stockholm: Swedish Nuclear Fuel and Waste Management Co. 58 pp.

Mantovani, M., Scherneck, H.-G., 2013. DInSAR investigation in the Pärvie end-glacial fault region, Lapland, Sweden. International Journal of Remote Sensing, 34 (23), pp. 8491-8502.

Wegmüller, U., Werner, C., Santoro, M., 2009. Motion monitoring for Etna using ALOS PALSAR time series. Proceedings, ALOS PI Symposium (pp. 9-13).